NUCLEAR PHYSICS B

Journal devoted to the experimental and theoretical study of the fundamental constituents of matter and their interactions

Nuclear Physics B226 (1983) 121–151

MIRROR LEPTONS

K. ENQVIST[1], K. MURSULA[2] and M. ROOS[2]

[1] *Research Institute for Theoretical Physics, University of Helsinki, Helsinki, Finland*
[2] *Department of High Energy Physics, University of Helsinki, Helsinki, Finland*

NORTH HOLLAND

AMSTERDAM

Nuclear Physics B226 (1983) 121–151

MIRROR LEPTONS

K. ENQVIST[1], K. MURSULA[2] and M. ROOS[2]

[1] *Research Institute for Theoretical Physics, University of Helsinki, Helsinki, Finland*
[2] *Department of High Energy Physics, University of Helsinki, Helsinki, Finland*

Received 25 November 1982
(Revised 21 March 1983)

We study the effects of the mixing of leptons and mirror leptons in charged current and neutral current processes at low energy. Expressions are derived for all relevant measurable quantities, taking into account various radiative constraints. We discuss the effects of the new phenomenon of neutrino–mirror-neutrino oscillations which may occur with light mirror neutrinos. Using a recent data set we determine the allowed ranges of the mixing angles and of $\sin^2\theta_w$ in several mixing models, distinguished by different assumptions on the mirror neutrino masses. We conclude that sizeable mixing is possible and that some mixing angles have a strong *negative* correlation with $\sin^2\theta_w$.

1. Introduction

Mirror leptons are leptons with V + A interactions, all other quantum numbers being the same as for ordinary leptons. The charged mirror leptons must be heavier than about 20 GeV since they have not been pair-produced at PETRA [1]. One also expects that they are lighter than a few hundred GeV, since their mass terms break $SU(2)_W \times U(1)_Y$ and also because they can affect radiatively the value of the parameter $\rho = (M_W^2/M_Z^2)\cos^2\theta_w$ which is known to be close to 1.0 [2].

Mirror leptons appear in many grand unified theories based on symmetry groups such as $SO(n > 10)$ [3,4], $SU(n > 5)$ [5] and E_8 [6]. In most of these theories the mirror leptons naturally obtain masses of the order of 100 GeV. Mirror leptons can also appear in composite models [7], and they may also be needed in globally supersymmetric theories with an extra U(1) group à la Fayet [8] to cancel axial anomalies connected with that group [9].

When mirror leptons mix with ordinary leptons, either via explicit Yukawa terms or radiatively [3], they change the chiral structure of weak currents. Charged currents acquire a small V + A component, while for neutral currents only the axial vector part will be modified. These changes might be detectable already at present energies. We study this possibility in this paper and we call our scheme "the mirror mixing model".

In the above mentioned theories there naturally appear mirror quarks as well as mirror leptons. However, for arguments detailed in subsect. 6.1, the effects of mirror quarks on low-energy weak interactions are expected to be negligibly small. In contrast, the effects of mixing ordinary leptons with mirror leptons can be much larger. For this reason we have undertaken first to derive expressions for the cross sections of all the relevant charged current (CC) and neutral current (NC) reactions including the effects of mirror leptons and then to make a statistical analysis to determine the range of mixing parameters allowed by the most recent data.

The present work extends earlier work [10–13] which concentrated exclusively on charged weak interactions.* The paper is organized as follows. In sect. 2 we recapitulate the main features of the mirror mixing model and review shortly the charged current sector. Sect. 3 contains the evaluation of constraints coming from some leptonic radiative processes. In sect. 4 we derive the theoretical formulas for the cross sections of processes involving purely leptonic neutral currents. Sect. 5 summarizes the τ family. In sect. 6 we consider lepton-hadron weak scattering as well as constraints arising from the absence of flavor changing neutral currents. Sect. 7 discusses the statistical analysis and presents the results of the fits. Finally, in sect. 8 we draw our conclusions.

2. The mirror mixing model

2.1. SOME BASIC DEFINITIONS

This model has been discussed extensively in refs. [10, 11]. The weak lagrangian in the mass eigenstate basis takes the following form:

$$\mathcal{L}^{\mathrm{CC}} = -\frac{g}{2\sqrt{2}} W_\mu^+ \sum_\ell \left\{ \bar{\psi}_{\nu_\ell} \gamma^\mu \left[R(\phi_\ell - \theta_\ell) - R(\phi_\ell + \theta_\ell)\gamma_5\tau_3 \right] \psi_\ell \right\} + \mathrm{h.c.},$$

$$\mathcal{L}^{\mathrm{NC}} = -\frac{g}{4\cos\theta_{\mathrm{w}}} Z_\mu \sum_\ell \left\{ \bar{\psi}_{\nu_\ell} \gamma^\mu \left[1 - R(2\phi_\ell)\gamma_5\tau_3 \right] \psi_{\nu_\ell} \right.$$

$$\left. + \bar{\psi}_\ell \gamma^\mu \left[4\sin^2\theta_{\mathrm{w}} - 1 + R(2\theta_\ell)\gamma_5\tau_3 \right] \psi_\ell \right\}, \tag{1}$$

where ψ_{ν_ℓ} and ψ_ℓ are given by

$$\psi_{\nu_\ell} = \begin{pmatrix} \nu_\ell \\ N_\ell \end{pmatrix}, \qquad \psi_\ell = \begin{pmatrix} \ell \\ L_\ell \end{pmatrix}. \tag{2}$$

* Similar studies have been done also within left-right symmetric models (see e.g. ref. [11] and references therein). However, as noted in ref. [11], the mirror mixing model leads to a different phenomenological structure of weak interactions from that of the LR models.

Capital letters denote mirror leptons. $R(\theta)$ is the 2×2 orthogonal mixing matrix. The particular V, A structure of the lagrangian (1) is a direct consequence of the rotation of chirality eigenstates to mass eigenstates. This rotation leaves the vector parts of neutral currents (including electromagnetic) unchanged.

In the following we sometimes use the notation [11]

$$V_\ell = \cos(\theta_\ell - \phi_\ell), \qquad \tilde{V}_\ell = \sin(\theta_\ell - \phi_\ell),$$

$$A_\ell = \cos(\theta_\ell + \phi_\ell), \qquad \tilde{A}_\ell = \sin(\theta_\ell + \phi_\ell), \tag{3}$$

$$\alpha_\ell = \frac{2V_\ell A_\ell}{V_\ell^2 + A_\ell^2},$$

$$\tilde{\alpha}_\ell = -\frac{2\tilde{V}_\ell \tilde{A}_\ell}{\tilde{V}_\ell^2 + \tilde{A}_\ell^2},$$

$$\beta_\ell = V_\ell A_\ell - \tilde{V}_\ell \tilde{A}_\ell, \tag{4}$$

It is known from e^+e^- experiments that charged mirror fermions must be heavier than about 20 GeV. Mirror neutrinos, however, may be light ($< m_e$) or heavy ($> m_K$).* Their couplings to the muon are known to be severely restricted for masses in the approximate range of 10 MeV and 200 MeV [14]. Therefore we will consider the following four extreme cases for the masses of mirror neutrinos of the first two generations:

model (a) $\quad m_{N_e}, m_{N_\mu} < m_e,$

model (b) $\quad m_{N_e} < m_e, m_{N_\mu} > m_K,$

model (c) $\quad m_{N_e}, m_{N_\mu} > m_K,$

model (d) $\quad m_{N_\mu} < m_e, m_{N_e} > m_K.$

Model (c) with heavy mirror neutrinos decoupled from low-energy phenomena also corresponds to the more general case that only ordinary fermions are present but with general V, A CC couplings and modified NC couplings.

We do not include the τ family in our complete analysis of the first two generations because of its limited and inaccurate data. In sect. 5 we consider the

* These bounds are somewhat optional and only reflect our choice of dealing with either light mirror neutrinos without any mass effects or heavy mirror neutrinos that do not appear in weak decays of pions and kaons.

third family separately, and only in the two cases when all the mirror neutrinos are either heavy or light. The few results that can be obtained for the τ family are given in sect. 7.

In models with light mirror neutrinos the neutrino beam produced in pseudoscalar or nuclear beta decay is a coherent superposition of the two mass eigenstates [11, 13]. This leads to an oscillating probability for finding an interacting neutrino or mirror neutrino. The phenomenon is analogous to the well-known case of flavor oscillations, but the additional novel feature is that now both chiralities interact. The rate of oscillations depends on the difference of the squared masses of neutrinos and mirror neutrinos, $\Delta m_\nu^2 = |m_{\mathrm{N}}^2 - m_\nu^2|$. However, as we will argue in sect. 3, in order not to contradict astrophysical constraints in these models, either the neutrino and mirror neutrino masses must be very small ($< 10^{-2}$ eV), or the mixing angle θ_ℓ must nearly vanish ($\theta_\ell \leqslant 10^{-5}$).

In the former case the very small neutrino and mirror neutrino masses guarantee that oscillations turn on very slowly. Actually, in all the scattering processes we consider, no sizeable oscillation happens before an interaction in the target. Therefore the scattering cross sections are now independent of the arbitrary mass difference and also of the respective neutrino mixing angle ϕ_ℓ. We call this *coherent* scattering.

In the latter case θ_ℓ is practically zero and we evade the mass restriction. Now, if $\phi_\ell \neq 0$, we have the possibility of a neutrino-mirror neutrino oscillation. However, the scattering cross sections are then in general dependent on the oscillating term which includes the unknown neutrino mass factor Δm_ν^2. Assuming that this mass factor is such that, in all scattering processes to be considered, neutrino-mirror neutrino oscillations are already well developed before the beam hits the detector, it follows that the oscillating term is averaged and the mass dependence drops out. The beam is then effectively an incoherent mixture of neutrino and mirror-neutrino mass eigenstates. Accordingly, we call this *incoherent* scattering.

This incoherent scattering is justified e.g. if m_{N} and m_ν are not accidentally degenerate and if the larger of them is at least of the order of 10 eV. In the following analysis we distinguish between coherent and incoherent scattering.

We still note that since weak scattering processes cannot differentiate between Dirac and Majorana neutrinos in the massless neutrino limit, we need not commit ourselves either way. However, it should be said that we have implicitly assumed the existence of $\mathrm{SU(2)_w} \times \mathrm{U(1)}$ singlet neutrinos $\nu_{\ell\mathrm{R}}$ and $\mathrm{N}_{\ell\mathrm{L}}$ (cf. eq. (1)).

2.2. CHARGED CURRENTS

Charged leptonic and hadronic currents in the mixing model have been studied in refs. [11, 13], respectively, and we refer the reader there for complete discussion. In the present paper we will use the same leptonic CC processes as in ref. [11].

The relevant CC quantities have been collected in tables 1–4. Table 1 lists the parameters in leptonic pseudoscalar decays and in nuclear beta decay in all the models. The well-known muon decay parameters are given in table 2, together with the electron longitudinal polarization P_{e^-}. Table 3 gives the cross section for inverse muon decay, normalized by its V − A expression. Finally, table 4 lists the experimental values as well as the V − A predictions of all these CC parameters.

TABLE 1
Formulas for the CC parameters coming from pseudoscalar and nuclear beta decay

Model	Parameter		
	R	P_{μ^-}	$-\frac{c}{v}P_{\beta^-}$
a	1	β_μ	β_e
b	$\frac{2}{V_\mu^2 + A_\mu^2}$	α_μ	β_e
c	$\frac{V_e^2 + A_e^2}{V_\mu^2 + A_\mu^2}$	α_μ	α_e
d	$\frac{1}{2}(V_e^2 + A_e^2)$	β_μ	α_e

TABLE 2
Formulas for the muon decay parameters

Model	Parameter				
	ρ	ξ	δ	P_{e^-}	G_F^2
a	$\frac{3}{8}(1 + \beta_e\beta_\mu)$	$2\beta_e - \beta_\mu$	$\frac{3}{8}\frac{\beta_e + \beta_\mu}{2\beta_e - \beta_\mu}$	$-\beta_e$	$\tilde{G}^2$
b	$\frac{3}{8}(1 + \beta_e\alpha_\mu)$	$2\beta_e - \alpha_\mu$	$\frac{3}{8}\frac{\beta_e + \alpha_\mu}{2\beta_e - \alpha_\mu}$	$-\beta_e$	$\frac{1}{2}\tilde{G}^2(V_\mu^2 + A_\mu^2)$
c	$\frac{3}{8}(1 + \alpha_e\alpha_\mu)$	$2\alpha_e - \alpha_\mu$	$\frac{3}{8}\frac{\alpha_e + \alpha_\mu}{2\alpha_e - \alpha_\mu}$	$-\alpha_e$	$\frac{1}{4}\tilde{G}^2(V_e^2 + A_e^2)(V_\mu^2 + A_\mu^2)$
d	$\frac{3}{8}(1 + \alpha_e\beta_\mu)$	$2\alpha_e - \beta_\mu$	$\frac{3}{8}\frac{\alpha_e + \beta_\mu}{2\alpha_e - \beta_\mu}$	$-\alpha_e$	$\frac{1}{2}\tilde{G}^2(V_e^2 + A_e^2)$

TABLE 3
Formulas for the inverse muon decay parameter S ($c = 0.375$)

Model	Parameter S
a	$\frac{1}{2}P_{\nu\nu}^{\mu}\{(\cos^4\theta_\mu + \sin^4\theta_\mu)(1 + c) + \beta_e(\cos^4\theta_\mu - \sin^4\theta_\mu)(1 - c)\}$
b	$\frac{1}{4}\{(1 + \alpha_\mu^2)(1 + c) + 2\beta_e\alpha_\mu(1 - c)\}$
c	$\frac{1}{4}\{(1 + \alpha_\mu^2)(1 + c) + 2\alpha_e\alpha_\mu(1 - c)\}$
d	$\frac{1}{2}P_{\nu\nu}^{\mu}\{(\cos^4\theta_\mu + \sin^4\theta_\mu)(1 + c) + \alpha_e(\cos^4\theta_\mu - \sin^4\theta_\mu)(1 - c)\}$

TABLE 4
The constraints used, their experimental values and their best fit values in the standard GWS theory and in one mixing model

Data set	Experimental quantity	Experimental value	GWS value at $\sin^2\theta_W = 0.239$	Best fit value in model (c)	Experimental reference
leptonic	ρ	0.7517 ± 0.0026	$\frac{3}{4}$	0.7496	21
CC	δ	0.7551 ± 0.0085	$\frac{3}{4}$	0.7511	21
	ξP_{μ^-}	0.9722 ± 0.0140	1	0.9981	21
	S	0.98 ± 0.12	1	1.002	40
	P_{e^-}	1.001 ± 0.008	1	0.999	41
	P_{μ^-}	0.99 ± 0.16	1	1.000	42
	$R_{\pi, K}$	1.016 ± 0.017	1	1.015	21
leptonic	$\langle \sigma(\bar{\nu}_e e^-) \rangle^{(i)}_{low}$	7.6 ± 2.2	5.580	5.064	23
NC	$\sigma(\bar{\nu}_\mu e^-)^{(ii)}$	1.54 ± 0.67	1.375	1.197	24
	$\sigma(\nu_\mu e^-)^{(ii)}$	1.46 ± 0.24	1.503	1.552	24
	$\sigma(\nu_\mu e^-)/\sigma(\bar{\nu}_\mu e^-)$	$1.37 \pm 0.65/-.44$	1.093	1.297	25
	A^{FB}(14 GeV)	$(2.6 \pm 3.0)\%$	-1.38%	-1.43%	26
	A^{FB}(22 GeV)	$(-6.9 \pm 3.4)\%$	-3.66%	-3.80%	26
	A^{FB}(34 GeV)	$(-11.9 \pm 1.5)\%$	-10.47%	-10.93%	26
	h_{VV}	0.009 ± 0.040	0.0005	0.0044	27
semi-leptonic	R_p	$0.47 \pm .064$	0.401	0.395	33
NC and CC	R_n	$0.22 \pm .031$	0.240	0.234	33
	R^-	$0.264 \pm .008$	0.261	0.264	34, 35
	R^+	$0.315 \pm .009$	0.325	0.313	35
semi-leptonic	$a_1(x)^{(iii)}$	-9.7 ± 2.6	-7.60	-8.66	36
NC	$a_2(x)^{(iii)}$	4.9 ± 8.1	-0.72	-2.21	36
	$B/F(y)Q^{2(iv)}$	-1.40 ± 0.35	-1.56	-1.54	37

The absolute values are given in units of: (i) 10^{-46} cm^2; (ii) 10^{-42} $E_{(\bar{\nu})}$ cm^2/GeV; (iii) 10^{-5} GeV^{-2}; (iv) 10^{-4} GeV^{-2}.

3. Constraints from leptonic radiative processes

Mixing of mirror fermions will also contribute to various physical properties of ordinary fermions through radiative corrections. These can then be used to set limits on the masses of mirror fermions or on their mixing angles. In this section we will focus on the radiative decay of neutrinos and on the mirror fermion contribution to the anomalous magnetic moments of ordinary leptons.

The relevant Feynman diagrams for both these processes are displayed in fig. 1. The external real photon couples to the magnetic form factors of these diagrams. We do not consider the Higgs sector of our mixing model in order to avoid model-dependent statements. Consequently we will neglect all Higgs-mediated processes, although they might be important for radiative corrections. If there exist charged

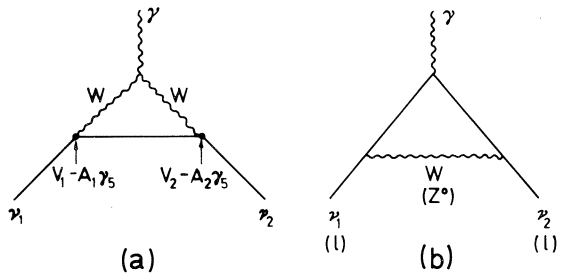

Fig. 1. The diagrams contributing both to radiative neutrino decay and the anomalous magnetic moment of the leptons.

physical higgses, they could have considerable effects, since their couplings to fermions are not necessarily as small as the ordinary Yukawa couplings are.

The calculation of the magnetic form factors $F_2^{(a)}$ and $F_2^{(b)}$ of the diagrams of fig. 1a and 1b, respectively, is straightforward [15] with external masses neglected in the Feynman integral. The result, which by itself is not gauge invariant but which gives the correct order of magnitude, is in the 't Hooft-Feynman gauge

$$F_2^{(a)} = \frac{\tilde{G}}{(4\pi)^2\sqrt{2}} 4m(m_1+m_2) f(\xi)\Gamma,$$

$$F_2^{(b)} = \frac{\tilde{G}}{(4\pi)^2\sqrt{2}} 3m(m_1+m_2) h(\xi)\Gamma, \tag{5}$$

where Γ is given by

$$\Gamma = V_1V_2 - A_1A_2 + (V_1A_2 - V_2A_1)\gamma_5, \tag{6}$$

and the coupling constants V_i, A_i $(i = 1,2)$ parametrize the two charged currents (see fig. 1). Here m is the mass of the internal fermion, m_1 and m_2 are the external fermion masses and $\xi = m^2/m_W^2$. The functions $f(\xi)$ and $h(\xi)$ are defined as follows:

$$f(\xi) = \frac{\xi \ln \xi - \frac{1}{2}(\xi^2 - 1)}{(1-\xi)^3},$$

$$h(\xi) = \frac{(\xi-1)^2 + \frac{1}{2}(\xi^2-1) - \xi^2 \ln \xi}{(1-\xi)^3}. \tag{7}$$

3.1. THE RADIATIVE DECAY

Let us consider first the dominant decay modes of mirror fermions. Heavy mirror fermions (both charged and neutral) will decay very rapidly to ordinary fermions through weak decay. The rate may be somewhat suppressed by the small mixing angles, but, on the other hand, it is enhanced by the large masses of mirror fermions.

The main decay mode of *light* mirror neutrinos as well as neutrinos is radiative decay $N_\ell \to \nu_\ell \gamma$ (or $\nu_\ell \to N_\ell \gamma$, whichever is kinematically allowed). The rate for the decay $N_\ell \to \nu_\ell \gamma$ is [16]

$$\Gamma(N_\ell \to \nu_\ell \gamma) = \frac{e^2 m_{N_\ell}}{8\pi}\left(1 - \frac{m_{\nu_\ell}}{m_{N_\ell}}\right)^2\left(1 - \frac{m_{\nu_\ell}^2}{m_{N_\ell}^2}\right)\left[|F_{2V}^{(a)} + F_{2V}^{(b)}|^2 + |F_{2A}^{(a)} + F_{2A}^{(b)}|^2\right], \tag{8}$$

where the vector and axial vector form factors $F_{2V}^{(k)}$ and $F_{2A}^{(k)}$ ($k = a, b$) are defined through $F_2^{(k)} \equiv F_{2V}^{(k)} + F_{2A}^{(k)}\gamma_5$ (see eqs. (5) and (6)).

In our case the main contribution to this rate comes from the diagrams with a heavy internal mirror fermion. From the lagrangian (1) and from eqs. (5) and (8) we obtain, assuming for simplicity that $m_{N_\ell} \gg m_{\nu_\ell}$ (the coupling constants are $V_1 = V_\ell$, $V_2 = \tilde{V}_\ell$, $A_1 = -A_\ell$ and $A_2 = \tilde{A}_\ell$):

$$\Gamma(N_\ell \to \nu_\ell \gamma) = \frac{\alpha \tilde{G}^2 m_{L_\ell}^2 m_{N_\ell}^3}{1024\pi^4}[4f(\xi) + 3h(\xi)]^2(1 + \cos^2 2\phi_\ell)\sin^2 2\theta_\ell. \tag{9}$$

The functions $f(\xi)$ and $h(\xi)$ vary slowly in the range $0.25 \leqslant m_{L_\ell}/M_W \leqslant 2$, which we take to be a reasonable guess for the charged mirror lepton mass [3]. Using the known upper limit $\theta_\ell < 15°$ [11] and assuming $m_N < 100$ eV, we obtain an absolute lower limit for the (mirror) neutrino lifetime:

$$\tau_N > (2\text{–}10) \times 10^9 \text{ s} \tag{10}$$

where the lower value corresponds to $m_{L_\ell} = 2M_W$ and the upper to $m_{L_\ell} = 0.25\ M_W$.

However, these exist severe astrophysical constraints on the lifetime of unstable neutrinos [17]. These come from the observed cosmic photon spectrum and the 3° K background radiation, and do not allow for the existence of light neutrinos with lifetimes less than about 10^{20} s. For long-lived neutrinos in the mass range 10–100 eV there are also limits coming from the observed galactic UV radiation [18]. Therefore, to conform with these limits we must assume that either the mixing angle θ_ℓ is extremely small ($\sin 2\theta_\ell < O(10^{-5})$) or the neutrinos N_ℓ and ν_ℓ are very light (or that mirror neutrinos are heavier than about 1 keV. However, we do not consider this last possibility here)*.

* There is another, but more model dependent, limit from the cosmological ^{4}He synthesis on the number of light, relatively stable ($\tau > 1$ s) neutrinos. This limit is saturated in our model (a) with light ($m_N \ll 100$ eV) mirror neutrinos already by the first two generations. In order not to break this limit in this particular submodel we have to assume that the subsequent neutrinos and mirror neutrinos are heavier than about 100 keV.

The first possibility to conform with these limits is to set θ_ℓ equal to zero. However, since ϕ_ℓ can still be large and since there are no very strict bounds on the masses of neutrinos and mirror neutrinos, neutrino-mirror neutrino oscillation is possible.

The second possibility is to set a strict upper bound on all light neutrino masses ($N = N_\ell, \nu_\ell$)

$$m_N \lesssim 2 \times 10^{-2}\,\mathrm{eV}. \tag{11}$$

This result implies that there will be no beam oscillations in laboratory neutrino scattering experiments as was discussed in subsect. 2.1. Furthermore, the corresponding neutrino mixing angle(s) ϕ_ℓ remain unrestricted.

3.2. THE ANOMALOUS MAGNETIC MOMENT

We now turn our attention to the anomalous magnetic moments of ordinary leptons. Because of their supposedly large masses the mirror fermions will give a considerable contribution to these moments. A straightforward application of eq. (5) gives for their effect on the anomaly a_ℓ

$$\Delta a_\ell = -\frac{\tilde{G} m_\ell^2}{8\pi^2\sqrt{2}}\left[2\frac{m_{L_\ell}}{m_\ell} f(\xi_1)\sin 2\theta_\ell + \frac{m_{N_\ell}}{m_\ell} h(\xi_2)\sin 2\phi_\ell\right] \times \sin 2\theta_\ell, \tag{12}$$

where $\xi_1 = m_{L_\ell}^2/M_W^2$ and $\xi_2 = m_{N_\ell}^2/M_W^2$ (and $m_{N_\ell} \gg m_\ell$; if this is not the case, one ignores the second term in eq. (12)). In contrast, the usual weak contribution in the GWS model is [19]

$$a_{GWS} = \frac{G_F m_\ell^2}{8\pi^2\sqrt{2}}\left[\tfrac{16}{3}\sin^4\theta_w - \tfrac{8}{3}\sin^2\theta_w + \tfrac{1}{4}\right].$$

The experimental error for the anomaly of the muon is [20] $\Delta a_\mu^{exp} = \pm 9 \times 10^{-9}$, and for that of the electron [21] $\Delta a_e^{exp} = \pm 2 \times 10^{-10}$. The ordinary weak contribution is not visible at present accuracies.

To get a rough idea of the range of mixing angles allowed by eq. (12) and by the experimental uncertainties, let us assume that $\phi_\ell \ll \theta_\ell$ and/or $m_{N_\ell} \ll m_{L_\ell}$. With the experimental lower limit on a new charged heavy lepton [1] $m_{L_\ell} > 20$ GeV, we obtain the limits

$$\theta_e < 9^\circ, \quad \theta_\mu < 10^\circ.$$

However, in the absence of a rigorous gauge-invariant treatment of the anomaly these figures should be taken as indicative of the order of magnitude only. Because the masses of the charged mirror fermions must be heavy, in a complete model there

might exist large Yukawa couplings, which could make the Higgs-induced contributions sizeable. The actual magnitude of all these contributions depends on many unknowns, such as the (model-dependent) number of physical charged higgses. All one can say as far as the anomalies are concerned, is that the mixing angles θ_ℓ should be smaller than O(10°).

Ordinary neutrinos, if massive, will also get a leading contribution to their anomalous magnetic moments from diagrams similar to those of fig. 1. The magnitude of this contribution will be of the order of $Gm_{\nu_\ell} m_{L_\ell} \times$ (mixing angle). This is smaller than the contribution Δa_ℓ to the charged lepton anomalous magnetic moment by a factor of m_{ν_ℓ}/m_ℓ.

4. Leptonic NC processes

4.1. GENERAL FORMALISM FOR ELASTIC $\bar{\nu}\ell$ SCATTERING

First we give a general expression for the cross section of a leptonic weak process $\bar{\ell}_1^0 \ell_2 \to \bar{\ell}_3^0 \ell_2$ with a general V, A structure for both the neutral vector boson t-channel exchange and the charged vector boson s-channel exchange (see fig. 2). Here $\bar{\ell}_1^0$ and $\bar{\ell}_3^0$ are neutral antileptons, and ℓ_2 is a charged lepton. We take also into account the non-trivial longitudinal polarization of the $\bar{\ell}_1^0$ beam, but we neglect the kinematical effects of the $\bar{\ell}_1^0$ and $\bar{\ell}_3^0$ masses.

We parametrize the matrix element as follows:

$$\mathcal{M} = \frac{\tilde{G}}{2\sqrt{2}} \bar{v}(q_1, s)\gamma^\mu (m - n\gamma_5) v(q_3) \bar{u}(q_2')\gamma_\mu (p + q\gamma_5) u(q_2)$$

$$\times \sqrt{\tfrac{1}{2}}\, \tilde{G} \bar{v}(q_1, s)\gamma^\mu (V - A\gamma_5) u(q_2) \bar{u}(q_2')\gamma_\mu (V' - A'\gamma_5) v(q_3). \qquad (13)$$

This yields the following differential cross section in the laboratory system

$$\frac{\mathrm{d}\sigma}{\mathrm{d}K_2} = \frac{m_2}{4\pi} \left\{ T_1 \left(1 - \frac{K_2}{E_1}\right)^2 + T_2 - T_3 \frac{m_2 K_2}{E_1^2} + T_4 \frac{K_2(K_2 + m_2)}{E_1^2} \right\}, \qquad (14)$$

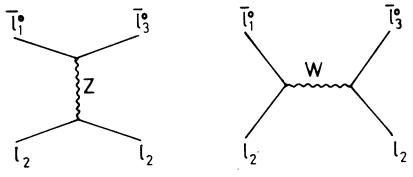

Fig. 2. The two tree-level contributions to a general neutral antilepton (charged lepton weak scattering).

where m_2, K_2 and E_1 are mass and the kinetic energy of the particle ℓ_2 in the final state and the initial energy of the particle $\bar{\ell}_1^0$, respectively. The fourth term in eq. (14) vanishes if pure V − A coupling is assumed for the charged current.

Factors T_i are combinations of the chiral coupling constants. Let us denote the longitudinal polarization of $\bar{\ell}_1^0$ by P_1. Then

$$T_1 = |G_{VV} + G_{AA}|^2 + |G_{VA} + G_{AV}|^2 - 2P_1\mathrm{Re}\left[(G_{VV} + G_{AA})(G_{VA}^* + G_{AV}^*)\right],$$

$$T_2 = |G_{VV} - G_{AA}|^2 + |G_{VA} - G_{AV}|^2 + 2P_1\mathrm{Re}\left[(G_{VV} - G_{AA})(G_{VA}^* - G_{AV}^*)\right],$$

$$T_3 = |G_{VV}|^2 + |G_{AV}|^2 - |G_{VA}|^2 - |G_{AA}|^2 - 2P_1\mathrm{Re}\left[G_{VV}G_{AV}^* - G_{VA}G_{AA}^*\right],$$

$$T_4 = |G_{SS}|^2 + |G_{SP}|^2 - 2P_1\mathrm{Re}\left[G_{SS}G_{SP}^*\right]. \tag{15}$$

The subscripts on the parameters G refer to the Lorentz structure of the two fermion currents in the effective NC process obtained by Fierz-transforming the CC part in eq. (13). The parameters G_{ij} are themselves combinations of coupling constants appearing in eq. (13). We list their expressions below:

$$G_{VV} = \frac{\tilde{G}}{2\sqrt{2}}\left[mp + VV' + AA'\right],$$

$$G_{AA} = \frac{\tilde{G}}{2\sqrt{2}}\left[-nq + VV' + AA'\right],$$

$$G_{VA} = \frac{\tilde{G}}{2\sqrt{2}}\left[mq - VA' - V'A\right],$$

$$G_{AV} = \frac{\tilde{G}}{2\sqrt{2}}\left[-np - VA' - V'A\right],$$

$$G_{SS} = \frac{\tilde{G}}{2\sqrt{2}}\left[-2VV' + 2AA'\right] = -G_{PP},$$

$$G_{SP} = \frac{\tilde{G}}{2\sqrt{2}}\left[-2VA' + 2V'A\right] = -G_{PS}. \tag{16}$$

These results can be applied fairly straightforwardly to all neutrino-electron scattering processes in the models (a)–(d). Let us first consider elastic $\bar{\nu}_e$e scattering.

4.2. ELASTIC $\bar{\nu}_e$e SCATTERING

4.2.1. Models (c) and (d). In these two models, the electron mirror neutrino N_e is heavy and thus decoupled from the low-energy scattering phenomena. The NC and CC coupling constants of eq. (13) are now given by

$$
\begin{aligned}
m &\equiv m_e = 1\,, \\
n &\equiv n_e = \cos 2\phi_e\,, \\
p &\equiv p_e = 4\sin^2\theta_w - 1\,, \\
q &\equiv q_e = \cos 2\theta_e\,, \\
V &= V' \equiv V_e = \cos(\theta_e - \phi_e)\,, \\
A &= A' \equiv A_e = \cos(\theta_e + \phi_e)\,,
\end{aligned}
\tag{17}
$$

and the polarization of $\bar{\nu}_e$ is $P_l = \alpha_e$, where α_e is given by eq. (4).

4.2.2. Models (a) and (b). These two models contain a light mirror neutrino N_e. As discussed in sect. 2 we have the two possibilities of coherent and incoherent neutrino scattering. We briefly mention how to calculate the cross section in both of these cases.

Let us first consider incoherent scattering. There the beam is an incoherent mixture of the two mass eigenstates $\bar{\nu}_e$ and $\overline{N}_e$. We then have the following four subprocesses which contribute to "elastic" $\bar{\nu}_e e^-$ scattering:

$$
\begin{aligned}
&\bar{\nu}_e e^- \to \bar{\nu}_e e^-\,, \qquad \bar{\nu}_e e^- \to \overline{N}_e e^-\,, \\
&\overline{N}_e e^- \to \bar{\nu}_e e^-\,, \qquad \overline{N}_e e^- \to \overline{N}_e e^-\,.
\end{aligned}
\tag{18}
$$

The coupling constants of eq. (13) for each of these subprocesses can be read off from the lagrangian (1) with $\theta_e = 0$. The polarizations of the beam particles are trivially ± 1 when θ_e vanishes and $\bar{\nu}_e$ and $\overline{N}_e$ appear in the beam with relative weights of $\cos^2\phi_e$ and $\sin^2\phi_e$, respectively.

In the case of coherent scattering the beam can be regarded effectively as an incoherent mixture of weak eigenstates $\bar{\nu}'_e$ and $\overline{N}'_e$ whose interactions are easily seen in weak currents written in a mixed basis of neutrino weak eigenstates and charged

lepton mass eigenstates:

$$J^{\mu}_{\mathrm{CC}} = -\frac{g}{2\sqrt{2}}\{\cos\theta_{\ell}\bar{\nu}'_{\ell}\gamma^{\mu}(1-\gamma_5)\ell - \sin\theta_{\ell}\bar{N}'_{\ell}\gamma^{\mu}(1+\gamma_5)\ell$$

$$+\sin\theta_{\ell}\bar{\nu}'_{\ell}\gamma^{\mu}(1-\gamma_5)L_{\ell} + \cos\theta_{\ell}\bar{N}'_{\ell}\gamma^{\mu}(1+\gamma_5)L_{\ell}\},$$

$$J^{\mu}_{\mathrm{NC}} = -\frac{g}{4\cos\theta_{\mathrm{w}}}\{\cos\theta_{\ell}\bar{\nu}'_{\ell}\gamma^{\mu}(1-\gamma_5)\nu_{\ell} - \sin\theta_{\ell}\bar{N}'_{\ell}\gamma^{\mu}(1+\gamma_5)\nu_{\ell}$$

$$+\sin\phi_{\ell}\bar{\nu}'_{\ell}\gamma^{\mu}(1-\gamma_5)N_{\ell} + \cos\phi_{\ell}\bar{N}'_{\ell}\gamma^{\mu}(1+\gamma_5)N_{\ell}\}. \tag{19}$$

As above, all the four subprocesses (18) with the incoming neutrinos being now the weak interaction eigenstates $\bar{\nu}'_{\mathrm{e}}$ and $\bar{\mathrm{N}}'_{\mathrm{e}}$ add up incoherently to the total cross section. The polarizations are trivial and the relative weights of $\bar{\nu}'_{\mathrm{e}}$ and $\bar{\mathrm{N}}'_{\mathrm{e}}$ in the beam are $\cos^2\theta_{\mathrm{e}}$ and $\sin^2\theta_{\mathrm{e}}$, respectively.

The final result for both coherent and incoherent scattering cross sections can be written in terms of T_i as follows:

$$T_1 = \tfrac{1}{2}\tilde{G}^2 P^{\mathrm{e}}_{\nu\nu}\{\cos^2\theta_{\mathrm{e}}(4\cos^2\theta_{\mathrm{e}} + p_{\mathrm{e}} - q_{\mathrm{e}})^2 + \sin^2\theta_{\mathrm{e}}(4\sin^2\theta_{\mathrm{e}} + p_{\mathrm{e}} - q_{\mathrm{e}})^2\},$$

$$T_2 = \tfrac{1}{2}\tilde{G}^2 P^{\mathrm{e}}_{\nu\nu}\{\cos^2\theta_{\mathrm{e}}(p_{\mathrm{e}} + q_{\mathrm{e}})^2 + \sin^2\theta_{\mathrm{e}}(p_{\mathrm{e}} - q_{\mathrm{e}})^2\},$$

$$T_3 = \tfrac{1}{2}\tilde{G}^2 P^{\mathrm{e}}_{\nu\nu}\{p_{\mathrm{e}}^2 - q_{\mathrm{e}}^2 + 4\cos^4\theta_{\mathrm{e}}(p_{\mathrm{e}} + q_{\mathrm{e}}) + 4\sin^4\theta_{\mathrm{e}}(p_{\mathrm{e}} - q_{\mathrm{e}})\},$$

$$T_4 = 8\tilde{G}^2 P^{\mathrm{e}}_{\nu\nu}\sin^2\theta_{\mathrm{e}}\cos^2\theta_{\mathrm{e}}, \tag{20}$$

where p_{e} and q_{e} are given in eq. (17). In the coherent scattering case $P^{\mathrm{i}}_{\nu\nu}$ ($i = \mathrm{e}, \mu$) is trivially 1, and in the incoherent case it is given by

$$P^{\mathrm{i}}_{\nu\nu} = 1 - \tfrac{1}{2}\sin^2 2\phi_{\mathrm{i}}. \tag{21}$$

Note that to apply eq. (20) in the incoherent case one has to put θ_{e} equal to zero. The scale of the cross sections is given by $\tilde{G}^2$ which is related to the measured Fermi constant G_{F}^2 as shown in table 2. Recall that in each model this relation is different.

4.2.3. Experimental considerations. In order to make contact with experiments we have to integrate the differential cross section (14) over the relevant values of K_2 and also average it over the estimated spectrum of reactor neutrinos. Using the spectrum given by Davis et al. [22] we find the following result for the two energy ranges of the electron (low: 1.5 MeV $\leqslant K_2 \leqslant$ 3.0 MeV; high: 3.0 MeV $\leqslant K_2 \leqslant$ 4.5

MeV)

$$\langle\sigma(\bar{\nu}_e e)\rangle_{\text{low}} = A\frac{\tilde{G}^2}{G_F^2}\{0.2760\tilde{T}_2 + 0.0401\tilde{T}_1 - 0.0298\tilde{T}_3 + 0.1520\tilde{T}_4\}, \quad (22)$$

$$\langle\sigma(\bar{\nu}_e e)\rangle_{\text{high}} = A\frac{\tilde{G}^2}{G_F^2}\{0.0725\tilde{T}_2 + 0.0045\tilde{T}_1 - 0.0063\tilde{T}_3 + 0.0493\tilde{T}_4\}, \quad (23)$$

where

$$A = \frac{m_e G_F^2}{32\pi}\ \text{MeV} = 2.6935 \times 10^{-46}\ \text{cm}^2,$$

$$\tilde{T}_i = 8T_i/\tilde{G}^2.$$

The numbers multiplying the factors $\tilde{T}_i$ $(i = 1, 2, 3)$ in eqs. (22) and (23) are well known and frequently used [2], but the ones multiplying $\tilde{T}_4$ have been obtained by an approximate treatment of the neutrino spectrum and are liable to small modifications. Still, they remain fairly large and positive. Therefore, this additional term which appears as soon as non-trivial charged currents are considered, could increase the theoretical cross section for elastic $\bar{\nu}_e e$ scattering. However, we can easily see from eq. (20) that in our models the terms $\tilde{T}_4$ remain very small and we cannot explain the persistent discrepancy between the theoretical cross sections and the Savannah River reactor experiments [23]:

$$\langle\sigma(\bar{\nu}_e e)\rangle_{\text{low}}^{\text{exp}} = (7.6 \pm 2.2) \times 10^{-46}\ \text{cm}^2, \quad (24)$$

$$\langle\sigma(\bar{\nu}_e e)\rangle_{\text{high}}^{\text{exp}} = (1.86 \pm 0.48) \times 10^{-46}\ \text{cm}^2. \quad (25)$$

In particular, the latter experimental result, eq. (25) is very sensitive to the poorly known high-energy tail of the antineutrino beam spectrum. As it is in serious conflict with other data we choose not to include it as a constraint.

4.3. ELASTIC $\bar{\nu}_\mu e$ AND $\nu_\mu e$ SCATTERING

These reactions proceed only through Z° exchange. Thus we can use the formulae of the two previous sections by setting $V = V' = A = A' = 0$ and changing the mixing angle ϕ_e to ϕ_μ. The electron mass terms in the cross section can now safely be neglected. The cross section for $\bar{\nu}_\mu e$ scattering can be written in all models as

$$\sigma(\bar{\nu}_\mu e) = A\left(\frac{E_{\bar{\nu}}}{\text{MeV}}\right)\frac{\tilde{G}^2}{G_F^2}\left(\tfrac{1}{3}\tilde{T}_1 + \tilde{T}_2\right), \quad (26)$$

while for the ν_μe scattering it is

$$\sigma(\nu_\mu e) = A\left(\frac{E_{\bar\nu}}{\text{MeV}}\right)\frac{\tilde G^2}{G_F^2}\left(\tfrac{1}{3}\tilde T_2 + \tilde T_1\right). \tag{27}$$

4.3.1. Models (b) and (c). These models assume a heavy muonic mirror neutrino, and $\tilde T_1$ and $\tilde T_2$ can be recast in the following simple form

$$\tilde T_1 = (mp - nq)^2 + (mq - np)^2 - 2\alpha_\mu(mp - nq)(mq - np), \tag{28}$$

$$\tilde T_2 = (mp + nq)^2 + (mq + np)^2 + 2\alpha_\mu(mp + nq)(mq + np), \tag{29}$$

where α_μ is given by eq. (4) and p, q and n are the same as in eq. (17), while $n = n_\mu = \cos 2\phi_\mu$.

4.3.2. Models (a) and (d). These models contain a light muonic mirror neutrino. The $\tilde T_i$ are given by

$$\tilde T_1 = 4P_{\nu\nu}^\mu\left[\cos^2\theta_\mu(p_e - q_e)^2 + \sin^2\theta_\mu(p_e + q_e)^2\right], \tag{30}$$

$$\tilde T_2 = 4P_{\nu\nu}^\mu\left[\cos^2\theta_\mu(p_e + q_e)^2 + \sin^2\theta_\mu(p_e - q_e)^2\right]. \tag{31}$$

Again we differentiate between the two possibilities allowed by neutrino radiative decay. In the coherent case $P_{\nu\nu}^\mu = 1$, and in the incoherent case $P_{\nu\nu}^\mu = 1 - \frac{1}{2}\sin^2 2\phi_\mu$ (and $\theta_\mu = 0$).

4.3.3. Experimental constraints. We take the experimental values from Mo [24], however, subtracting out the (then preliminary) cross sections of the CHARM experiment:

$$\sigma^{\exp}(\bar\nu_\mu e) = (1.54 \pm 0.67)\times 10^{-42} E_{\bar\nu}\,\frac{\text{cm}^2}{\text{GeV}}, \tag{32}$$

$$\sigma^{\exp}(\nu_\mu e) = (1.46 \pm 0.24)\times 10^{-42} E_{\bar\nu}\,\frac{\text{cm}^2}{\text{GeV}}. \tag{33}$$

From the CHARM experiment [25] we take the cross section ratio

$$\frac{\sigma^{\exp}(\nu_\mu e^-)}{\sigma^{\exp}(\bar\nu_\mu e^-)} = 1.37^{+0.65}_{-0.44}. \tag{34}$$

4.4. NC EFFECTS IN $e^+e^- \to \mu^+\mu^-$

The formal expression for the differential cross section $(d\sigma/d\Omega)(e^+e^- \to \mu^+\mu^-)$ is the same for all the models considered in this paper. It is given by

$$\frac{d\sigma}{d\Omega}(e^+e^- \to \mu^+\mu^-) = \frac{\alpha^2}{4s}\left[F_1(s)(1 + \cos^2\theta) + F_2(s)\cos\theta\right], \tag{35}$$

where

$$F_1(s) = 1 + 2p_e p_\mu X(s) + \left(p_e^2 + q_e^2\right)\left(p_\mu^2 + q_\mu^2\right) Y(s),$$

$$F_2(s) = 4q_e q_\mu \left[X(s) + 2p_e p_\mu Y(s)\right]. \tag{36}$$

The vector and axial vector NC coupling constants p_i and q_i of lepton i have the form presented in eq. (17). In the zero-width approximation the functions $X(s)$ and $Y(s)$ are given by

$$X(s) \simeq \frac{s}{16\sin^2\theta_w \cos^2\theta_w \left(s - m_Z^2\right)},$$

$$Y(s) \simeq X^2(s). \tag{37}$$

The forward-backward asymmetry A^{FB} is then easily obtained from eq. (35):

$$A^{FB} = \frac{3}{8}\frac{F_2(s)}{F_1(s)}. \tag{38}$$

The Z-boson mass in eq. (37) is related to M_W and $\tilde{G}$ in a well known way. Let us again remind the reader that in all our models the relation of $\tilde{G}$ to the measured Fermi constant G_F is different. This produces also slight differences to A^{FB}, although the expressions are formally the same.

For the experimental input we use the averaged values [26] given for three energy regions (mean $\sqrt{s}$ = 14, 22 and 34 GeV):

$$A_{exp}^{FB}(14\ \text{GeV}) = (2.6 \pm 3.0)\%,$$

$$A_{exp}^{FB}(22\ \text{GeV}) = (-6.9 \pm 3.4)\%,$$

$$A_{exp}^{FB}(34\ \text{GeV}) = (-11.9 \pm 1.5)\%. \tag{39}$$

There exists also separate information on the coefficient of the $(1 + \cos^2\theta)$ term in eq. (35) coming from the quantity

$$\frac{\sigma - \sigma_{QED}}{\sigma_{QED}} = \frac{4sG_F}{\sqrt{2}\,e^2} h_{VV}.$$

In our models, we have

$$h_{VV} = \frac{\tilde{G}}{G_F}\frac{1}{4}\left(1 - 4\sin^2\theta_w\right)^2. \tag{40}$$

We use the experimental average of PETRA measurements [27]

$$h_{VV}^{exp} = 0.009 \pm 0.040, \tag{41}$$

as an additional constraint furnishing information on the weak mixing angle θ_w.

5. The τ family

Although we mainly concentrate on the complete analysis of the first two generations, a few comments on the third family can be made. Since the τ data are still far less informative than the data for e- and μ-families, they do not appreciably affect the values and limits of the e- and μ-parameters, but only poorly limit the angles θ_τ and ϕ_τ. Consequently, we do not consider the full set of mixing models for the τ family. We use the existing τ data to determine limits to θ_τ and ϕ_τ in two sample models: one with all mirror neutrinos (nearly) massless and the other with all of them very massive. The limits to θ_τ and ϕ_τ are calculated from experimental errors only while keeping the parameters θ_e, ϕ_e, θ_μ and ϕ_μ at their best fit values.

We only have two pieces of information available: the ρ-parameter for $\tau \to e\nu\nu$ decay and the charge asymmetry A^{FB} in the reaction $e^+e^- \to \tau^+\tau^-$. The e/μ decay ratio of the τ is trivial in the first case and in the second case it only depends on the mixing angles of the first two families. All other data depend on hadronic coupling constants and cannot be used.

The theoretical expressions for ρ_τ and $A^{FB}(\tau)$ are easily obtained from their analogues in table 2 and eqs. (35) to (38). In the case of light mirror neutrinos only θ_τ is restricted, ϕ_τ remains arbitrary. In the second model ρ_τ depends also on ϕ_τ and both angles are restricted. Experiments at PETRA give the following values [28, 26]:

$$\rho_\tau = 0.72 \pm 0.15, \tag{42}$$

$$A^{FB} = (-6.8 \pm 2.8)\%, \qquad \text{at mean } \sqrt{s} = 34\,\text{GeV}. \tag{43}$$

6. Lepton-hadron weak scattering

6.1. RADIATIVE CONSTRAINTS

The most accurate data on the weak mixing angle θ_w comes, as is well known, not from the purely leptonic processes but from ν_μN scattering data. Therefore it is desirable to extend the mirror mixing scheme also to hadrons. However, we then immediately face considerable complications of a practical nature. In principle, each quark flavor would have its own mixing angle, and thus the number of parameters would be doubled, at least. This unwanted proliferation of coupling parameters would render any analysis useless. However, we will argue in the following that

possible quark-mirror quark mixing angles must be so small that they have no observable effect on the weak processes and can be set equal to zero in the following analysis.

Flavor mixing is an essential feature of quark weak currents. When extending the theory to mirror-quark mixing it is obvious that the subtle cancellation of flavor changing neutral currents (FCNC) due to the GIM mechanism is lost. In the most general case FCNC arise already at the tree level. According to a recent general analysis [29] of the first two generations, the observed absence of FCNC sets an upper bound of the order of 10^{-3} to the mirror mixing angles of the quark sector.

Even if the flavor changing neutral currents were absent at the tree level, they can be induced by radiative corrections. To check what this implies for the quark mixing angles, we consider the case where Cabibbo mixing is equal for quarks and mirror quarks. Then the FCNC are absent at the tree level by virtue of the GIM mechanism. The NC lagrangian reads

$$\mathcal{L}_{\mathrm{NC}} \sim \left(\bar{\Psi}_{\mathrm{u}}\gamma_\mu \Gamma_1 \Psi_{\mathrm{u}} + \bar{\Psi}_{\mathrm{c}}\gamma_\mu \Gamma_2 \Psi_{\mathrm{c}} + \cdots\right) z^\mu . \tag{44}$$

The fields

$$\Psi_{\mathrm{u}} = \begin{pmatrix} \mathcal{U} \\ \mathcal{D}' \end{pmatrix}, \qquad \Psi_{\mathrm{c}} = \begin{pmatrix} \mathcal{C} \\ \mathcal{S}' \end{pmatrix}, \ldots$$

are doublets under weak SU(2) and $\mathcal{U} = \begin{pmatrix} \mathrm{u} \\ \mathrm{U} \end{pmatrix}$, where u is an ordinary quark and U a mirror quark (similarly for $\mathcal{D}'$, $\mathcal{C}$, $\mathcal{S}'$ etc.). The primes in $\mathcal{D}'$, $\mathcal{S}'$, ... denote that they are Cabibbo-rotated states:

$$\begin{pmatrix} \mathcal{D}' \\ \mathcal{S}' \\ \vdots \end{pmatrix} = U_{\mathrm{C}} \begin{pmatrix} \mathcal{D} \\ \mathcal{S} \\ \vdots \end{pmatrix}. \tag{45}$$

The operator Γ_i contains the chiral structure of the coupling and e.g. Γ_1 is given by

$$\Gamma_1 = \begin{pmatrix} v_{\mathrm{u}} \otimes \mathbb{1} & 0 \\ 0 & v_{\mathrm{d}} \otimes \mathbb{1} \end{pmatrix} + \begin{pmatrix} a_{\mathrm{u}} \otimes \sigma_3 & 0 \\ 0 & a_{\mathrm{d}} \otimes \sigma_3 \end{pmatrix} \gamma_5 , \tag{46}$$

and only the axial vector couplings are modified by mixing ($a_i = \cos(2\theta_i) a_i^{\mathrm{WS}}$).

As an example of the magnitude of FCNC induced by radiative corrections we consider the $\mathrm{K}^0 - \overline{\mathrm{K}}^0$ mass difference due to the box diagram in fig. 3. The charged current lagrangian is analogous to the leptonic lagrangian of eq. (1). Let us assume for the sake of argument that all quark-mirror quark mixings are roughly of the same magnitude; we denote this angle θ_{q}. The effective lagrangian for the induced

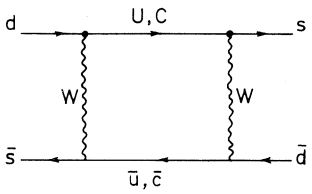

Fig. 3. Example of a box diagram giving rise to flavor changing neutral currents.

$K^0 - \overline{K}^0$ mass difference obtained from fig. 3 is then

$$\mathcal{L}_{\text{eff}} \sim \sqrt{\tfrac{1}{2}}\,\tilde{G}\frac{\alpha}{2\pi}\frac{\sin^2 2\theta_q}{\sin^2\theta_w}\bar{d}\left[4\gamma_\rho(1-\gamma_5)+\gamma_\rho(1+\gamma_5)\right]s\bar{s}\gamma^\rho(1-\gamma_5)\,d$$

$$\times\frac{1}{1-x}\left[1+\frac{x}{1-x}\ln x\right]\sin^2\theta_C\cos^2\theta_C, \tag{47}$$

where $x = m_Q^2/M_W^2$ (m_Q is a "typical" mass of the mirror quarks). Let us put $x = 1$ for simplicity. We demand that the effective coupling of eq. (47) is smaller than the corresponding coupling obtained from the usual GIM mechanism [30]. Direct comparison to experiments is not straightforward because K-mesons are bound states. However, this method does give a rough order of magnitude, which is what we need:

$$\sin^2 2\theta_q \lesssim O(10^{-1})\frac{m_c^2}{M_W^2}. \tag{48}$$

Here m_c is the mass of the ordinary charmed quark, and the factor $O(10^{-1})$ arises from constant factors in eq. (47). Eq. (48) then implies that only very small quark mixing angles, $\theta_q \lesssim O(10^{-4})$, are allowed.

To conclude, there appear no flavor changing neutral currents, neither at tree level nor radiatively induced, provided the quark-mirror quark mixing is less than $O(10^{-4})$. Mixing angles of this order of magnitude have no observable effect in our analysis of weak processes. Therefore in the following we will neglect all mirror mixings in the quark sector and thus the quark weak interactions are those of the standard GWS model.

6.2. NEUTRINO HADRON SCATTERING

6.2.1. Models (b) and (c). We start by giving the differential CC cross sections for (anti)neutrino-quark scattering (neglecting the quark masses)

$$\frac{d\sigma_{CC}}{dx\,dy}\left(\overset{(-)}{\nu}_{\mu q}\right) = \frac{\tilde{G}^2\left(V_\mu^2+A_\mu^2\right)}{8\pi}sxu_q(x)\left\{\left(1\underset{(-)}{+}\alpha_\mu\right)^2+\left(1\underset{(+)}{-}\alpha_\mu\right)^2(1-y)^2\right\}, \tag{49}$$

where $u_q(x)$ is the quark x distribution and α_μ is the polarization of the incoming antineutrino, given by eq. (4).* Relating $\tilde{G}^2$ to G_F^2 (table 2) one sees that in model (b) all the differences between eq. (43) and the V − A expression are due to the non-trivial polarization α_μ. However, in model (c) there also appears a new factor $2(V_e^2 + A_e^2)^{-1}$ in the differential cross section. This dependence of the muon neutrino scattering on the coupling constants of the electron generation may seem surprising. It shows how intimately the two generations are connected through G_F in this kind of model.

Similarly, for the differential NC cross section we obtain

$$\frac{d\sigma_{NC}}{dx\,dy}\left({}^{(-)}_{\mu q}\right) = \frac{\tilde{G}^2\left(1+\cos^2 2\phi_\mu\right)}{16\pi} sx u_q(x)$$
$$\times\left\{\left(g_V^2+g_A^2\right)(1+\alpha_\mu\gamma)\left[1+(1-y)^2\right]\right.$$
$$\left.{}^{(\mp)}\,2g_V g_A(\gamma+\alpha_\mu)\left[1-(1-y)^2\right]\right\}, \tag{50}$$

where g_V and g_A are the NC coupling constants of the quark current, the same as in the standard GWS model. The parameter γ is given by

$$\gamma = \frac{2\cos 2\phi_\mu}{1+\cos^2 2\phi_\mu}. \tag{51}$$

In eq. (50) we have tacitly assumed that the mirror neutrino N_μ is so heavy that it cannot be produced by present neutrino beam energies.

As we will discuss later in sect. 7 we know on the basis of this analysis that all the mixing angles which can be determined are small enough to allow us to expand eqs. (49) and (50) in terms of them. (We choose to expand to the second power.) Then we easily obtain the corresponding cross sections for an arbitrary nuclear target N:

$$\sigma_{CC}\left({}^{(-)}_{\mu}N\right) = \frac{\tilde{G}^2}{G_F^2} k_{CC}\sigma_{CC}^{V-A}\left({}^{(-)}_{\mu}N\right),$$

$$\sigma_{NC}\left(\nu_\mu N\right) = \frac{\tilde{G}^2}{G_F^2}\left\{k^1_{NC}\sigma_{NC}^{V-A}\left(\nu_\mu N\right) + k^2_{NC}\sigma_{NC}^{V-A}\left(\bar{\nu}_\mu N\right)\right\},$$

$$\sigma_{NC}\left(\bar{\nu}_\mu N\right) = \frac{\tilde{G}^2}{G_F^2}\left\{k^1_{NC}\sigma_{NC}^{V-A}\left(\bar{\nu}_\mu N\right) + k^2_{NC}\sigma_{NC}^{V-A}\left(\nu_\mu N\right)\right\}, \tag{52}$$

* Using the most recent data on the y distribution of high-energy νN charged current scattering it has been shown [13] that the additional y-dependent terms in the CC cross section (due to the non-trivial polarization) do not yield more restrictive constraints on the leptonic mixing angles than already obtained from low-energy CC data [11].

where the correction factors for models (b) and (c) are

$$k_{CC} = V_\mu A_\mu \simeq 1 - \theta_\mu^2 - \phi_\mu^2,$$

$$k_{NC}^1 = \tfrac{1}{8}(1 + \cos 2\phi_\mu)^2 \frac{(V_\mu + A_\mu)^2}{V_\mu^2 + A_\mu^2} \simeq 1 - 2\phi_\mu^2,$$

$$k_{NC}^2 = \tfrac{1}{8}(1 - \cos 2\phi_\mu)^2 \frac{(V_\mu - A_\mu)^2}{V_\mu^2 + A_\mu^2} \simeq 0. \tag{53}$$

We use the data on isoscalar targets $\overline{N}$ in the form of the very practical Paschos-Wolfenstein relation [31]

$$R^- = \frac{\sigma_{NC}(\nu_\mu \overline{N}) - \sigma_{NC}(\bar{\nu}_\mu \overline{N})}{\sigma_{CC}(\nu_\mu \overline{N}) - \sigma_{CC}(\bar{\nu}_\mu \overline{N})} = r^- R_{V-A}^-, \tag{54}$$

and the similar ratio [32] for the sums

$$R^+ = \frac{\sigma_{NC}(\nu_\mu \overline{N}) + \sigma_{NC}(\bar{\nu}_\mu \overline{N})}{\sigma_{CC}(\nu_\mu \overline{N}) + \sigma_{CC}(\bar{\nu}_\mu \overline{N})} = r^+ R_{V-A}^+. \tag{55}$$

Both of these ratios are practically independent of the quark distribution functions with their V − A values given as follows

$$R_{V-A}^+ = \tfrac{1}{2} - \sin^2\theta_w + \tfrac{10}{9}\sin^4\theta_w,$$

$$R_{V-A}^- = \tfrac{1}{2} - \sin^2\theta_w. \tag{56}$$

Furthermore, the correction factors $r^\pm$ are calculable exactly (without expansion), and they are

$$r^- = \frac{1}{2}\left[\frac{\cos 2\phi_\mu}{V_\mu A_\mu} + \frac{1 + \cos^2 2\phi_\mu}{V_\mu^2 + A_\mu^2}\right] \simeq 1 + \theta_\mu^2 - \phi_\mu^2,$$

$$r^+ = \frac{(V_\mu^2 + A_\mu^2)(1 + \cos^2 2\phi_\mu) + 4\cos 2\phi_\mu V_\mu A_\mu}{(V_\mu^2 + A_\mu^2)^2 + 4V_\mu^2 A_\mu^2} \simeq 1 + \theta_\mu^2 - \phi_\mu^2. \tag{57}$$

Moreover we use data on inclusive (anti)neutrino scattering on protons and neutrons. This data is expressed in terms of the ratios

$$ {}^{(-)}R_{\mathrm{N}} = \frac{\sigma_{\mathrm{NC}}\left({}^{(-)}\nu_{\mu}\mathrm{N}\right)}{\sigma_{\mathrm{CC}}\left({}^{(-)}\nu_{\mu}\mathrm{N}\right)}, \tag{58} $$

Using eq. (52) one easily finds the relations

$$ \begin{aligned} R_{\mathrm{N}} &= \left(k^{1}_{\mathrm{NC}}/k_{\mathrm{CC}}\right) R_{\mathrm{N}}^{\mathrm{V-A}} + \left(k^{2}_{\mathrm{NC}}/k_{\mathrm{CC}}\right) \bar{R}_{\mathrm{N}}^{\mathrm{V-A}} S_{\mathrm{N}}^{\mathrm{V-A}}, \\ \bar{R}_{\mathrm{N}} &= \left(k^{1}_{\mathrm{NC}}/k_{\mathrm{CC}}\right) \bar{R}_{\mathrm{N}}^{\mathrm{V-A}} + \left(k^{2}_{\mathrm{NC}}/k_{\mathrm{CC}}\right) R_{\mathrm{N}}^{\mathrm{V-A}}/S_{\mathrm{N}}^{\mathrm{V-A}}, \end{aligned} \tag{59} $$

where

$$ S_{\mathrm{N}} = S_{\mathrm{N}}^{\mathrm{V-A}} = \frac{\sigma_{\mathrm{CC}}\left(\bar{\nu}_{\mu}\mathrm{N}\right)}{\sigma_{\mathrm{CC}}\left(\nu_{\mu}\mathrm{N}\right)}. \tag{60} $$

However, now the corresponding ratios in the V − A limit ($ {}^{(-)}\bar{R}_{\mathrm{N}}^{\mathrm{V-A}} $ and $ S_{\mathrm{N}}^{\mathrm{V-A}} $) depend explicitly on the quark distribution functions (and experimental conditions). The usual parametrization, e.g., for the ratio $ R_{\mathrm{N}}^{\mathrm{V-A}} $ is [2, 32]

$$ R_{\mathrm{N}}^{\mathrm{V-A}} = f_1^{\mathrm{N}} u_{\mathrm{L}}^2 + f_2^{\mathrm{N}} d_{\mathrm{L}}^2 + f_3^{\mathrm{N}} u_{\mathrm{R}}^2 + f_4^{\mathrm{N}} d_{\mathrm{R}}^2, \tag{61} $$

where the factors $ f_i $ contain the above mentioned dependence on quark distributions and experimental conditions and the parameters $ u_{\mathrm{L,R}} $ and $ d_{\mathrm{L,R}} $ are the well known chiral NC coupling constants of quarks [32].

Similar equations could be derived also for (quasi)elastic (anti)neutrino scattering on protons or neutrons. However, for reasons discussed later in subsect. 6.2 (iii), we neglect these data.

6.2.2. Models (a) and (d). The corresponding differential CC cross sections are

$$ \begin{aligned} \frac{\mathrm{d}\sigma_{\mathrm{CC}}}{\mathrm{d}x\,\mathrm{d}y}\left({}^{(-)}\nu_{\mu}\mathrm{N}\right) = P^{\mu}_{\nu\nu}\frac{\tilde{G}^2}{2\pi} s x u_{\mathrm{q}}(x)\Big\{ &\cos^4\theta_{\mu} + \sin^4\theta_{\mu} \; {}^{(+)}_{(-)}\left(\cos^4\theta_{\mu} - \sin^4\theta_{\mu}\right) \\ &+ \left[\cos^4\theta_{\mu} + \sin^4\theta_{\mu} \; {}^{(-)}_{(+)}\left(\cos^4\theta_{\mu} - \sin^4\theta_{\mu}\right)\right](1-y)^2\Big\}, \end{aligned} \tag{62} $$

and the NC cross sections are

$$ \begin{aligned} \frac{\mathrm{d}\sigma_{\mathrm{NC}}}{\mathrm{d}x\,\mathrm{d}y}\left({}^{(-)}\nu_{\mu}\mathrm{N}\right) = P^{\mu}_{\nu\nu}\frac{\tilde{G}^2}{4\pi} s x u_{\mathrm{q}}(x)\Big\{ &\left(g_{\mathrm{V}}^2 + g_{\mathrm{A}}^2\right)\left[1 + (1-y)^2\right] \\ &{}^{(-)}_{(+)}\, 2 g_{\mathrm{V}} g_{\mathrm{A}} \cos 2\theta_{\mu}\left[1 - (1-y)^2\right]\Big\}. \end{aligned} \tag{63} $$

After expanding the above cross sections in terms of small angles (effectively, dropping the extra contribution to the differential CC cross section) one gets the total cross sections again to the form of eq. (52), where the correction factors are now

$$k_{\mathrm{CC}} = P^{\mu}_{\nu\nu}\cos^4\theta_\mu \simeq P^{\mu}_{\nu\nu}\left(1-2\theta_\mu^2\right),$$

$$k^1_{\mathrm{NC}} = P^{\mu}_{\nu\nu}\cos^2\theta_\mu \simeq P^{\mu}_{\nu\nu}\left(1-\theta_\mu^2\right),$$

$$k^2_{\mathrm{NC}} = P^{\mu}_{\nu\nu}\sin^2\theta_\mu \simeq P^{\mu}_{\nu\nu}\theta_\mu^2. \tag{64}$$

Also the correction factors of the relations (54) and (55) are easily calculated:

$$r^+ = \left[\cos^4\theta_\mu + \sin^4\theta_\mu\right]^{-1} \simeq 1 + 2\theta_\mu^2,$$

$$r^- = \frac{\cos 2\theta_\mu}{\cos^4\theta_\mu - \sin^4\theta_\mu} \simeq 1. \tag{65}$$

We note in passing that it would be valuable to have accurate information on the absolute scale of the (either differential or total) NC cross sections

$$\Sigma = \sigma_{\mathrm{NC}}\left(\nu_\mu N\right) + \sigma_{\mathrm{NC}}\left(\bar{\nu}_\mu N\right) = K\frac{\tilde{G}^2}{G_{\mathrm{F}}^2}\Sigma_{\mathrm{V-A}}. \tag{66}$$

For models (b) and (c), $K = \frac{1}{4}(1+\cos^2\phi_\mu)(1+\alpha_\mu\gamma)$, whereas for models (a) and (d), $K = P^{\mu}_{\nu\nu}$. Since $\sin^2\theta_{\mathrm{w}}$ is mostly determined by the ratios (54) and (55) the absolute scale Σ measures e.g. in model (a) just the oscillation factor $P^{\mu}_{\nu\nu}$.

6.2.3. Experimental constraints. Although there are five measurements of R_{p}, two of R_{n} and one of $\overline{R}_{\mathrm{p}}$ we can make use only of those experiments that report also the values of the constraints f_i (eq. (61)) including their errors. This restricts us to use only two measurements for one experiment [33]

$$R_{\mathrm{p}} = 0.47 \pm 0.064, \qquad R_{\mathrm{n}} = 0.22 \pm 0.031. \tag{67}$$

Here the errors of the constants f_i have been propagated to the experimental errors of R_{p} and R_{n}.

For the Paschos-Wolfenstein ratio R^- the results of four experiments [34, 35] can be combined to yield

$$R^- = 0.264 \pm 0.008. \tag{68}$$

The CFRR group [35] has also reported a value of R^+ which we can use:

$$R^+ = 0.315 \pm 0.009. \tag{69}$$

For elastic scattering there are four measurements of R_{e1}^{p}, one of $\bar{R}_{e1}^{p}$ and one of R_{e1}^{n}. None of these experiments have evaluated the relevant constants f_i with errors. We therefore refrain from using them in the present work.

6.3. CHARGE ASYMMETRIES IN POLARIZED LEPTON-HADRON SCATTERING

6.3.1. Electron on deuterium. The asymmetry $A_D(x, y)$ is defined as

$$A_D(x, y) = \frac{d\sigma(e_R^-) - d\sigma(e_L^-)}{d\sigma(e_R^-) + d\sigma(e_L^-)} . \tag{70}$$

Dividing out its proportionality on Q^2 we find for all the mixing models

$$\frac{A_D(x, y)}{Q^2} = \frac{3\tilde{G}}{5\sqrt{2}\,\pi\alpha}\left[\left(C_{1u} - \tfrac{1}{2}C_{1d}\right) + \left(C_{2u} - \tfrac{1}{2}C_{2d}\right)F(y)\right], \tag{71}$$

where the y-dependent function is $F(y) = (1-(1-y)^2)/(1+(1-y)^2)$ and the coupling constants are

$$\begin{aligned} C_{1u} &= \left(\tfrac{4}{3}\sin^2\theta_w - \tfrac{1}{2}\right)\cos 2\theta_e , \\ C_{2u} &= 2\sin^2\theta_w - \tfrac{1}{2} , \\ C_{1d} &= \left(-\tfrac{2}{3}\sin^2\theta_w + \tfrac{1}{2}\right)\cos 2\theta_e , \\ C_{2d} &= -C_{2u} . \end{aligned} \tag{72}$$

Rewriting eq. (71) in the form $A_D(x, y)/Q^2 = a_1(x) + a_2(x)F(y)$ we can then compare the theoretical formulas with the results of the SLAC experiment [36]:

$$a_1(x) = (-9.7 \pm 2.6) \times 10^{-5}\ \text{GeV}^{-2}, \qquad a_2(x) = (4.9 \pm 8.1) \times 10^{-5}\ \text{GeV}^{-2}, \tag{73}$$

6.3.2. Muon on carbon. There also exists a recent result for the asymmetry B from μC scattering [37] where

$$B(P_1, P_2) = \frac{d\sigma(\mu^+, P_1) - d\sigma(\mu^-, P_2)}{d\sigma(\mu^+, P_1) + d\sigma(\mu^-, P_2)} , \tag{74}$$

The expression valid for B in all mixing models is

$$B(-P, P) = -\frac{3}{4}\frac{3\tilde{G}}{5\sqrt{2}\,\pi\alpha}\left[\cos 2\theta_\mu + P\left(4\sin^2\theta_w - 1\right)\right]F(y)Q^2 . \tag{75}$$

The experimental value is (with $P = 0.81$):

$$\frac{B(-P,P)}{F(y)Q^2} = -(1.40 \pm 0.35) \times 10^{-4}\ \mathrm{GeV}^{-2}. \tag{76}$$

7. Results of the fits

The values of the mixing angles have been determined previously [11, 12] using leptonic CC data alone. As noted in ref. [11] there are two reasons for extending the analysis to neutral currents. One is that some NC processes already have the same level of experimental accuracy as the CC reactions and therefore they help to determine the mixing parameters, at the cost of introducing only one additional parameter, $\sin^2\theta_w$.

The other reason is that some NC processes make restrictions on the mixing angles beyond what the CC data do. As found in ref. [11], the CC data leave the V − A limit in model (c) arbitrary in the sense that many non-trivial values of mixing angles give the V − A predictions. Now, the inclusion of NC data resolves this problem. For example e^+e^- asymmetry measures essentially the product $\cos 2\theta_\mu \cdot \cos 2\theta_e$, and the $(\bar{\nu}_\mu)$e scattering depends on $\cos 2\phi_\mu$. Thus the predictions of the standard GWS theory (including the V − A structure in the CC sector) are obtained in model (c) only when all the mixing angles vanish.

Furthermore, as noted in ref. [11], since the CC data do not involve any scattering experiment with $(\bar{\nu}_e)$ beams, the corresponding neutrino mixing angle ϕ_e is left arbitrary in models (a) and (b). Including now the elastic $\bar{\nu}_e$e scattering in the analysis we get also ϕ_e constrained in models (a) and (b) with incoherent scattering.

For completeness we shall use both the purely leptonic data set and the total leptonic and semi-leptonic data set. We call *semi-leptonic* those constraints which à priori would depend on quark parameters (which we, however, have taken to be trivial because of reasons discussed in subsect. 6.1). The constraints used and their experimental values are tabulated in table 4.

We group the models we have tested into four classes.

(i) Models (a), (b) and (d) with coherent neutrino scattering (call them $(a)_{coh}$, $(b)_{coh}$, $(d)_{coh}$). The respective neutrino mixing angle(s) ϕ_ℓ remain(s) undetermined.

(ii) The same models with incoherent neutrino scattering ($(a)_{inc}$, $(b)_{inc}$, $(d)_{inc}$). In this case, as explained in subsect. 3.1, the corresponding charged lepton mixing angle(s) θ_ℓ must be vanishingly small. This implies a non-universal V − A structure for charged currents and the standard NC couplings for charged leptons. However, neutrino mixing angles ϕ_ℓ can now be restricted.

(iii) The general 5-parametric model (c) and the two 3-parametric special cases: model $(c)_{V-A}$ where the charged lepton mixing angles are set to zero and model $(c)_{univ}$ where the universality constraints $\theta_e = \theta_\mu$ and $\phi_e = \phi_\mu$ are imposed.

(iv) The standard (universal) GWS model. In all models we find that the mirror mixing angles are consistent with zero, although their best values may differ from zero. We tabulate in table 5 for each angle its best fit value and, in brackets, the 68.3% upper confidence limit. This confidence limit corresponds to the requirement that all the non-vanishing mixing angles are simultaneously within their confidence limits, however θ_w is allowed to assume any value. In the mixing models we therefore do not give any errors for $\sin^2\theta_w$. For the standard GWS model we use another procedure: since θ_w is then the only free parameter we give it with its usual 1σ error.

To give an idea of the variation of $\sin^2\theta_w$ allowed in the mixing models, we plot in fig. 4 the contour of the simultaneous 68.3% confidence region of all the 5 parameters in model (c) projected onto the $(\sin^2\theta_w, \phi_\mu)$ plane. (Then the upper limits of the mixing parameters are about 12% larger than in table 5).

We review now briefly the results presented in table 5. First of all, the leptonic data set tends to give a somewhat larger value of $\sin^2\theta_w$ than the total data set both for the GWS model as well as for the mixing models. For the mixing angles both data sets give similar values, except for model (c).

Secondly, the effect of mixing on $\sin^2\theta_w$ is to *decrease* it. This can particularly be seen in models (b) and (c) where the largest best fit values for the mixing angles are obtained. The value of $\sin^2\theta_w$ in the standard model is

$$\sin^2\theta_w = 0.239 \pm 0.007 .$$

The reason for this value being about 1σ higher than in other global fits of NC data [2, 38] is that we have used the data on inclusive (anti)neutrino scattering on isoscalar targets (which determines $\sin^2\theta_w$ most accurately) in the Paschos-Wolfenstein form.

TABLE 5
Best fit values of the parameters (and their 1σ upper limits)

Model	Data set	$\sin^2\theta_w$	$\lvert\theta_e\rvert$	$\lvert\phi_e\rvert$	$\lvert\theta_\mu\rvert$	$\lvert\phi_\mu\rvert$	$\chi^2/\langle\chi^2\rangle$
a_{coh}	all	0.239	2.3° (< 3.8°)	–	0° (< 2.5°)	–	13.10/18
b_{coh}	all	0.232	2.3° (< 4.1°)	–	0° (< 9.0°)	8.4° (< 12.8°)	12.08/18
d_{coh}	all	0.239	0° (< 7.4°)	0° (< 8.2°)	0° (< 3.0°)	–	14.74/18
a_{inc}	all	0.239	0	0° (< 27.5°)	0	5.5° (< 16.3°)	13.80/18
b_{inc}	all	0.232	0	0° (< 36.3°)	0° (< 9.3°)	8.4° (< 12.9°)	12.84/18
d_{inc}	all	0.239	0° (< 7.4°)	0° (< 8.0°)	0	5.5° (< 18.2°)	14.69/18
c	leptonic	0.234	6.5° (< 16.7°)	18.6° (< 28.9°)	0° (< 19.8°)	20.8° (< 30.1°)	7.98/10
c	all	0.218	6.1° (< 16.4°)	11.5° (< 20.5°)	0.1° (< 13.2°)	14.5° (< 21.9°)	11.88/17
c_{V-A}	all	0.223	0	10.1° (< 17.8°)	0	12.5° (< 19.0°)	12.34/19
c_{univ}	all	0.223	3.2° (< 10.0°)	0° (< 8.0°)	$=\theta_e$	$=\phi_e$	13.00/19
GWS	leptonic	$0.247^{+.035}_{-.029}$	0	0	0	0	10.55/14
GWS	all	$0.239 \pm .007$	0	0	0	0	14.74/21

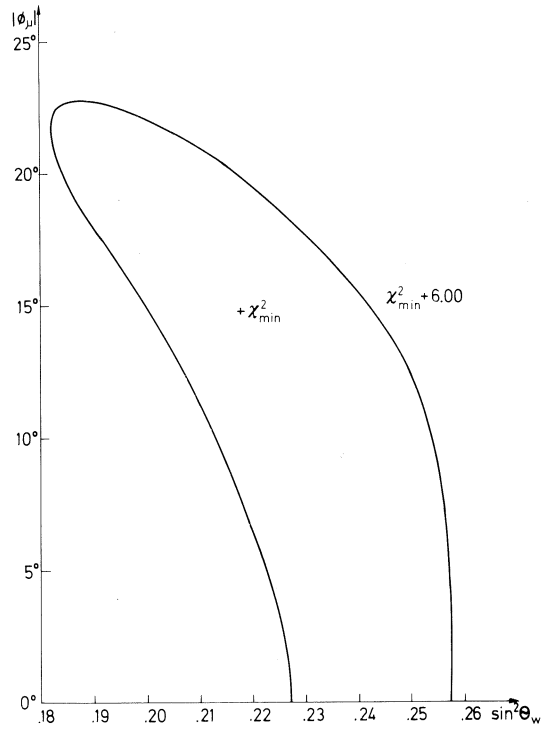

Fig. 4. Contour of the simultaneous 68.3% confidence region of all 5 parameters of model (c) projected onto the $(\sin^2\theta_w, |\phi_\mu|)$ plane. (See sect. 7).

Thirdly, the charged lepton mixing angles are much more constrained (in coherent models) than the neutrino mixing angles (in incoherent models). This leaves the possibility of large neutrino-mirror neutrino oscillations valid. Note that in coherent models one or two ϕ_ℓ's remain totally unrestricted.

Finally, the inclusion of NC data in addition to CC (see ref. [11]) has only slightly modified the values and limits of the mixing angles of models (a), (b) and (d). However, model (c) is now much better determined. This is due to the resolution of the above mentioned multiple V − A limit problem of CC data. As an example we show in table 4 the best fit values of all constraints in model (c) using the total data set.

Having found the best fit values of the e and μ mixing angles we have made a separate analysis for the τ mixing angles in the two sample models discussed in sect. 5. For the case of light mirror neutrinos there is no constraint on ϕ_τ and the upper limit for $|\theta_\tau|$ is:

$$|\theta_\tau| \leqslant 25^\circ .$$

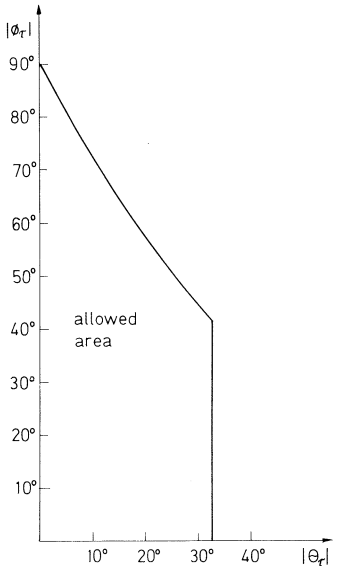

Fig. 5. The allowed area of the τ-parameters for the case of heavy mirror neutrinos.

For heavy mirror neutrinos the $\tau^+\tau^-$ asymmetry gives the upper limit:

$$|\theta_\tau| \leqslant 33^\circ ,$$

and the data on ρ_τ gives the contour of the allowed area in the $(|\theta_\tau|, |\phi_\tau|)$ plane. This area is depicted in fig. 5.

8. Conclusions

Mirror fermions appear in many theories based on large gauge symmetries, as discussed in sect. 1. Their effects through mixing with ordinary fermions on low-energy CC and NC processes have been analyzed in this work.

We note that in order to suppress the flavor changing neutral currents, the mixing in the quark sector must be vanishingly small (subsect. 6.1). However, no such constraint exists for the leptons, not even from the highly accurate data on the anomalous magnetic moments of the electron and muon (subsect. 3.2). Therefore we have concentrated on the mixing effects in the leptonic sector.

We parametrize the mixing in terms of charged and neutral lepton mixing angles θ_ℓ and ϕ_ℓ. We also consider various possibilities for the masses of the mirror neutrinos. In particular, we make a complete classification of the masses of the mirror neutrinos for the case of two generations. These correspond to the possibilities of having either a light ($< m_e$) or massive ($> m_K$) electron or muon mirror neutrino. We call these models (a), (b), (c) and (d) (see subsect. 2.1). Of these models

the model (c) can be interpreted in more general terms than within the mirror mixing model. It corresponds to any model where the charged currents have a general V, A structure (see also [11]) and the neutral currents have a modified axial vector part. We also comment on the status of the third family in two sample cases of light and heavy mirror neutrinos.

We argue in subsect. 3.1 that various astronomical limits from the cosmic photon spectrum and the 3 °K background radiation put severe constraints on the models with light mirror neutrinos. These constraints can be evaded in two ways. Either the (mirror) neutrinos are very light ($< 10^{-2}$ eV) or the charged lepton mixing angle θ_ℓ is negligible ($< 10^{-5}$). In the first case neutrino-mirror neutrino oscillation, which is possible if mirror neutrinos are light, can not be seen in present experiments since it has not yet started. The beam is completely coherent and we call this the coherent case.

In the other case θ_ℓ is zero and this leads to a (non-universal) V − A structure for the charged currents and to standard NC couplings for charged leptons. However, now neutrino-mirror neutrino oscillation is possible. In principle, the oscillation phenomena are dependent on the unknown neutrino mass term, but for simplicity, we discuss here only the possibility that the beam is oscillating rapidly and is therefore effectively incoherent. We call this case incoherent scattering.

We have then proceeded to analyze the various models described above in order to determine the mixing angles and $\sin^2\theta_w$. We use altogether 7 CC and 15 NC constraints in the fit. Their experimental values and best fits to the standard GWS theory and one of the mixing models are shown in table 4. Table 5 gives the best fit values and 1σ errors of the mixing angles in all the models we consider.

We now summarize the main features of the results presented in tables 4 and 5 and figs. 4 and 5.

(i) Including the mixing between leptons and mirror leptons seems to *decrease* $\sin^2\theta_w$. However, this change is not very large for the allowed range of mixing angles. As an example we show the $1\sigma(|\phi_\mu|, \sin^2\theta_w)$ contour of model (c) in fig. 4.

(ii) The mixing models (a), (b) and (c) give as good fits to the data as the standard GWS model. Model (d) was found to be less probable already on the basis of CC data [11].

(iii) The electron and muon mixing angles θ_e and θ_μ seem to be much more restricted than the angles ϕ_e and ϕ_μ of the corresponding neutrinos, where values up to 35° are allowed. This leaves much room for possible neutrino-mirror neutrino oscillations.

(iv) The largest deviations for most mixing angles are found in model (c).

(v) The τ angles are still poorly determined. For light mirror neutrinos only θ_τ is constrained ($|\theta_\tau| < 25°$) and ϕ_τ is free. If the mirror neutrinos are heavy a large area in the $(|\theta_\tau|, |\phi_\tau|)$ plane is allowed, as shown in fig. 5.

(vi) The allowed ranges of the mixing angles in many models are so large that they may, for example, allow an explanation of the persistent e/μ non-universality

implied by beam-dump experiments. This analysis will be done in a separate publication [39].

We want to thank Dr. J. Maalampi, CERN, for former collaboration on the charged current reactions. One of us (K.E.) thanks the Emil Aaltonen foundation for a grant.

References

[1] K.H. Mess and B.H. Wiik, preprint DESY 82-011 (1982), unpublished
[2] I. Liede and M. Roos, Nucl. Phys. B167 (1980) 397
[3] K. Enqvist and J. Maalampi, Nucl. Phys. B191 (1981) 189
[4] M. Ida, Y. Kayama and T. Kitazoe, Prog. Theor. Phys. 64 (1980) 1745;
J. Maalampi and K. Enqvist, Phys. Lett. 97B (1980) 217;
R. N. Mohapatra and B. Sakita, Phys. Rev. D21 (1980) 1062;
H. Sato, Phys. Lett. 101B (1981) 233;
F. Wilczek and A. Zee, Phys. Rev. D25 (1982) 553
[5] N.S. Baaklini, Phys. Rev. D21 (1980) 1932;
J. Chakrabarti, M. Popović and R.N. Mohapatra, Phys. Rev. D21 (1980) 3212;
C.W. Kim and C. Roiesnel, Phys. Lett. 93B (1980) 343;
Z.-q. Ma, T.-s. Tu, P.-y. Xue and X.-j. Zhou, Phys. Lett. 100B (1981) 399;
I. Umemura and K. Yamamoto, Phys. Lett. 100B (1981) 34;
M. Chaichian, Yu.N. Kolmakov and N.F. Nelipa, Phys. Rev. D25 (1982) 1377;
J.C. Pati, A. Salam and J. Strathdee, Phys. Lett. 108B (1982) 121
[6] I. Bars and M. Günaydin, Phys. Rev. Lett. 45 (1980) 859
[7] M. Chaichian, Yu.N. Kolmakov and N.F. Nelipa, Helsinki University preprint HU-TFT 82-15 (1982), unpublished
[8] P. Fayet, Phys. Lett. 69B (1977) 489; 84B (1979) 416
[9] P. Fayet, Proc. 17th Recontre de Moriond on elementary particles ed. J. Tran Thanh Van, Gif-sur-Yvette (Editions Frontiers, 1982) p. 483
[10] K. Enqvist, K. Mursula, J. Maalampi and M. Roos, Helsinki University preprint HU-TFT-81-18 (1981), unpublished
[11] J. Maalampi, K. Mursula and M. Roos, Nucl. Phys. B207 (1982) 233
[12] S. Nandi, A. Stern and E.C.G. Sudarshan, Phys. Rev. D26 (1982) 2522
[13] J. Maalampi and K. Mursula, Z. Phys. C16 (1982) 83
[14] Y. Asano et al., Phys. Lett. 104B (1981) 84;
R. Abela et al., SIN preprint PR 81-06 (1981)
[15] T.-P. Cheng and L.-F. Li, Phys. Rev. D16 (1977) 1425
[16] W.J. Marciano and A.I. Sanda, Phys. Lett. 67B (1977) 622
[17] F.W. Stecker and R.W. Brown, NASA preprint 83873 (1981), unpublished, and references therein
[18] A. de Rújula and S.L. Glashow, Phys. Rev. Lett. 45 (1980) 942
[19] W.A. Bardeen, R. Gastmans and B.E. Lautrup, Nucl. Phys. B46 (1972) 319
[20] J. Bailey et al., Nucl. Phys. B150 (1979) 1
[21] M. Roos et al., Phys. Lett. 111B (1982) 1
[22] B.R. Davis et al., Phys. Rev. C19 (1979) 2259
[23] F. Reines, H.S. Gurr and H.W. Sobel, Proc. Int. Neutrino Conf., Aachen, 1976 (Vieweg, Braunschweig, 1977) p. 217; Phys. Rev. Lett. 37 (1976) 315
[24] L.W. Mo, in Neutrino physics and astrophysics, ed. Ettore Fiorini (Plenum, New York, 1982) p. 191
[25] M. Jonker et al., Phys. Lett. 105B (1981) 242; Phys. Lett. 117B (1982) 272
[26] P. Steffen, DESY preprint DESY 82-039 (1982), unpublished
[27] F. Niebergall, Proc. Int. Conf. Neutrino '82 (Balatonfüred, 1982) vol. 2, p. 62 (Budapest, 1982)

[28] W. Bacino et al., Phys. Rev. Lett. 42 (1979) 749
[29] I. Umemura and K. Yamamoto, Phys. Lett. 108B (1982) 37
[30] M.K. Gaillard and B.W. Lee, Phys. Rev. D10 (1974) 897
[31] E.A. Paschos and L. Wolfenstein, Phys. Rev. D7 (1973) 91
[32] P.Q. Hung and J.J. Sakurai, Phys. Lett. 63B (1976) 295
[33] T. Kafka et al., Phys. Rev. Lett. 48 (1982) 910
[34] M. Holder et al., Phys. Lett. 72B (1977) 254;
C. Geweniger, Proc. Int. Neutrino Conf., Bergen, 1979 (Åstvedt Industrier Als, 1979) vol. 2, p. 392;
M. Jonker et al., Phys. Lett. 99B (1981) 265
[35] R. Blair et al., Proc. Int. Neutrino Conf., Hawaii, 1981 vol. I, p. 311
[36] C.Y. Prescott et al., Phys. Lett. 84B (1979) 524
[37] A. Argento et al., Phys. Lett. 120B (1983) 245
[38] J.E. Kim, P. Langacker, M. Levine and H.H. Williams, Rev. Mod. Phys. 53 (1980) 211
[39] K. Enqvist, K. Mursula and M. Roos, Helsinki University preprint HU-TFT-83-10 (1983)
[40] M. Jonker et al, Phys. Lett. 93B (1980) 203;
F. Bergsma et al., Phys. Lett. 122B (1983) 465
[41] F.W. Koks and J. von Klinken, Nucl. Phys. A272 (1976) 61
[42] R. Abela et al., Nucl. Phys. A395 (1983) 413